FEBS Letters 586 (2012) 384–391

journal homepage: www.FEBSLetters.org

PEDV ORF3 encodes an ion channel protein and regulates virus production

Kai Wang [a,1], Wei Lu [a,1], Jianfei Chen [c,1], Shiqi Xie [a], Hongyan Shi [c], Haojen Hsu [d], Wenjing Yu [a], Ke Xu [a], Chao Bian [b], Wolfgang B. Fischer [d], Wolfgang Schwarz [e,f], Li Feng [c,*], Bing Sun [a,b,*]

[a] Key Laboratory of Molecular Virology and Immunology, Institut Pasteur of Shanghai, Shanghai Institutes for Biological Sciences, Chinese Academy of Sciences, Shanghai 200025, China
[b] Laboratory of Molecular Cell Biology, Institute of Biochemistry and Cell Biology, Shanghai Institute of Biological Sciences, Chinese Academy of Sciences, 320 Yueyang Road, Shanghai 200031, China
[c] Division of Swine Infectious Diseases, National Key Laboratory of Veterinary Biotechnology, Harbin Veterinary Research Institute, Chinese Academy of Agricultural Sciences, 427 Maduan Street, Harbin 150001, China
[d] Institute of Biophotonics, School of Biomedical Science and Engineering, National Yang-Ming University, 155 Sec. 2, Li-Nong Street, Taipei 112, Taiwan, China
[e] Max-Planck-Institute for Biophysics, Max-von-Laue-Str. 3, D-60438 Frankfurt am Main, Germany
[f] Shanghai Research Center for Acupuncture and Meridian, 199 Guoshoujing Road, Shanghai 201203, China

ARTICLE INFO

Article history:
Received 21 November 2011
Revised 29 December 2011
Accepted 4 January 2012
Available online 11 January 2012

Edited by H.-D. Klenk

Keywords:
PEDV
ORF3
Ion channel
Molecular dynamics

ABSTRACT

Several studies suggest that the open reading frame 3 (ORF3) gene of porcine epidemic diarrhea virus (PEDV) is related to viral infectivity and pathogenicity, but its function remains unknown. Here, we propose a structure model of the ORF3 protein consisting of four TM domains and forming a tetrameric assembly. ORF3 protein can be detected in PEDV-infected cells and it functions as an ion channel in both *Xenopus laevis* oocytes and yeast. Mutation analysis showed that Tyr170 in TM4 is important for potassium channel activity. Furthermore, viral production is reduced in infected Vero cells when ORF3 gene is silenced by siRNA. Interestingly, the ORF3 gene from an attenuated PEDV encodes a truncated protein with 49 nucleotide deletions, which lacks the ion channel activity.
© 2012 Federation of European Biochemical Societies. Published by Elsevier B.V. All rights reserved.

1. Introduction

Porcine epidemic diarrhea virus (PEDV) is an enveloped single-stranded RNA virus that causes diarrhea in pigs of all ages and fatality in neonates [1]. The virus is a member of the family Coronaviridae and outbreaks causing heavy economic losses have been reported in many swine-raising countries such as Europe and Asia [2], despite the use of vaccines. In some countries such as China, damage caused by PEDV infection is continuous and serious.

The pattern of a potential gene located between the S and E genes is conserved in all three groups of coronavirus genomes. Only the genomes of SARS-CoV, HCoV-NL63 and PEDV have one complete ORF in this locus, whereas the genes in five other coronaviruses are truncated with only short ORFs due to mutations [3]. The ORF3 gene of several coronaviruses, including transmissible gastroenteritis virus (TGEV), can be recognized with insertions and deletions suggesting this area of the genome may be involved in viral pathogenicity [4].

Studies have shown that the ORF3 gene of PEDV has unexpected genetic variability [5]. For example, wild-type and cell culture adapted PEDV have almost complete sequence identity, with the exception of variations and truncations in the ORF3 gene [5–9]. The function of the ORF3 gene product in PEDV is unknown.

We have previously demonstrated that SARS-CoV ORF3 encodes a novel structural protein 3a that forms an ion channel and modulates virus release [10]. Based on the similarity in the genome organization between SARS-CoV and PEDV, we predict that the ORF3 protein of PEDV may have a similar function as SARS-CoV 3a. Here, we adapted the methods used for SARS-CoV 3a (10) to generate a computational model of PEDV ORF3 protein. We detect its potassium ion channel activity using *Xenopus laevis* oocytes and a potassium uptake-deficient strain of *Saccharomyces cerevisiae*. We show that virus production is reduced when using siRNA to knockdown ORF3 expression during PEDV infection. In vivo experiments also show that the existence of full length ORF3 is associated with pathogenesis. We thus demonstrate that the ORF3 protein of PEDV functions as an ion channel and enhances virus production.

Abbreviations: PEDV, porcine epidemic diarrhea virus; ORF, open reading frame; TGEV, transmissible gastroenteritis virus; ORi, oocyte Ringer's-like solution; TEVC, two electrode voltage clamp; TM, transmembrane; TMD, transmembrane domain; MD, molecular dynamics; sgRNA, subgenomic mRNA; MOI, multiplicity of infection

* Corresponding authors. Address: Key Laboratory of Molecular Virology and Immunology, Institut Pasteur of Shanghai, Shanghai Institutes for Biological Sciences, Chinese Academy of Sciences, 225 South Chongqing Road, Shanghai 200025, China. Fax: +86 21 63843571 (B. Sun), fax: 0451 85935073 (L. Feng).
E-mail addresses: fl@hvri.ac.cn (L. Feng), bsun@sibs.ac.cn (B. Sun).
[1] These authors contributed equally to this work.

0014-5793/$36.00 © 2012 Federation of European Biochemical Societies. Published by Elsevier B.V. All rights reserved.
doi:10.1016/j.febslet.2012.01.005

2. Materials and methods

2.1. Viruses and cells

Vero cells were maintained in Dulbecco's modified Eagle's essential medium supplemented with 10% fetal bovine serum and cultured at 37 °C in a humidified atmosphere with 5% CO_2. Wild type PEDV CV777 was provided by M. Pensaert (Gent Belgium) and passaged 3 times in colostrum-deprived piglets [11]. Attenuated PEDV was obtained from serial passaged Vero cells. The virus was cultured in Vero cells supplemented by Eagle's minimal essential medium (EMEM, Invitrogen, Carlsbad, USA) containing 10 μg/ml trypsin (Invitrogen) following Hofmann and Wyler [12]. Briefly, stock virus was inoculated to a confluent monolayer of Vero cells and placed at 37 °C and 5% CO_2. After 48–72 h, progeny virions were harvested and passaged for 147 passages in Vero cells until use as the vaccine strain against PEDV [13].

2.2. Plasmid DNA and antibodies

The PEDV ORF3 gene was cloned into a T-tailed vector, pMD18-T (TaKaRa Biotechnology Co. Ltd., Dalian, China) according to manufacturer instructions. The DNA clone was sequenced by Shanghai Sangon Biological Engineering Technology & Services Co. Ltd. (Shanghai, China). At the C terminus of the ORF3 protein sequence, a HA tag was added and cloned into pCAGGS-PEDV-HA (pCAGGS vector was kindly provided by Jun-ichi Miyazaki, Osaka University). The ORF3-EGFP fusion protein expression plasmid pEGFP-ORF3 was constructed by cloning the ORF3 gene into plasmid pEGFP-C1 (Clontech, Mountain View, USA). Three deletions (82-98del, 118-139del, 151-172del) were introduced into PEDV ORF3 plasmids constructed by QuikChange mutagenesis kit (Stratagene, La Jolla, USA). PEDV ORF3 gene was cloned into pYES2 plasmid (provided by Song Wei, Shanghai Institute of Biological Sciences) for yeast complementation assays. Monoclonal antibody anti-HA and polyclonal antibody anti-actin were purchased from Santa Cruz Biotechnology (Santa Cruz, USA). The polyclonal antibody anti-PEDV ORF3 was obtained from the Antibody Research Center (Shanghai Institute of Biochemistry and Cellular Biology, Chinese Academy of Sciences). This polyclonal antibody was custom-produced against synthetic peptide (VVKDVSKSVNLSLDAVQELEL) derived from the PEDV CV777 ORF3 protein.

2.3. Computational method

The approach to derive structural data for the assembly of viral membrane proteins within a two dimensional lipid bilayer environment has been described previously [14].

2.4. Western blot

Vero cells were infected with PEDV at a multiplicity of infection (MOI) of 0.1 for 48 h. Virus-infected and mock-infected cells were collected and lysed in sodium dodecyl sulfate (SDS) sample buffer (60 mM Tris–HCl (pH 6.8), 2% SDS, 10% glycerol, 5% 2-mercaptoethanol, 0.01% bromophenol blue), followed by boiling for 5 min. Western blotting was carried out as previously described [10].

2.5. Electrophysiology

The ORF3 cDNA was cloned into pNWP vector downstream of a SP6 promoter used for mRNA in vitro transcription. PCR products were digested with restriction enzymes SalI and BglII and ligated into the plasmid. ORF3 cRNA was synthesized by the mMESSAGE mMACHINE high-yield capped RNA transcription SP6 kit (Ambion, Austin, USA) and injected into *X. laevis* oocytes (10 ng per oocyte). Oocytes were obtained and prepared as previously described [15]. Forty-eight hours after injection, oocytes were used for electrophysiology and immunofluorescence. Two-electrode voltage clamp (TEVC) equipment (Turbo TEC 10, NPI Electronic, Tamm, Germany) was used to record currents from the plasma membrane of *Xenopus* oocytes with or without expressed ORF3 protein. The standard voltage-clamp protocol consisted of rectangular voltage steps of 300 ms. Steady-state I-V dependencies were from −150 to +30 mV in 10 mV increments applied from a holding voltage of −60 mV. Microelectrodes were filled with 3 M KCl and had a resistance of 0.5–1 MΩ. The oocytes were superfused at room temperature (approximately 22 °C) with standard bath solution (ORi containing 90 mM NaCl, 2 mM KCl, 2 mM $CaCl_2$, and 5 mM Hepes (pH 7.4)). The experimental solution comprised 100 mM KCl, 1.8 mM $CaCl_2$, 1 mM $MgCl_2$ and 5 mM Hepes (pH 7.4).

2.6. S. cerevisiae complementation assays

Yeast potassium uptake complementation experiments were performed [16]. The PEDV ORF3 gene was transformed into W303 yeast strain R5421 (ura3-52 his3Δ200 leu2 Δ1 trp1 Δ1 ade2 trk1 Δ::HIS3 trk2 Δ::HIS3) (from Richard F. Gaber, Northwestern University) deficient in endogenous K^+ uptake systems (trk1 and trk2 mutations). Yeasts from the same stock were grown in parallel under non-selective conditions on YNB plates supplemented with 100 mM KCl and on selective conditions on normal YNB medium without additional K^+. Growth experiments were performed at 30 °C.

2.7. siRNA knockdown

The design of siRNA that can specifically knockdown genes encoded by targeted sgRNA has been described elsewhere [17]. According to the convention [18], we design a PCR forward primer CCTTGTCTACTCAATTCAAC, to amplify and subsequently to determine the sequence of junction sites of the subgenomic mRNA species. However, the leader-mRNA junction of the ORF3 subgenomic mRNA between the wild PEDV and attenuated PEDV was the same, different from Tobler and Ackermann [18]. The siRNA target sequence (TGCAGTGATGTTTCTTGGA) was chosen according to criteria previously described [19] and chemically synthesized by Ribobio (Guangzhou, China). siRNA sequence: sense 5′UGCAGUGAUGUUUCUUGGAdTdT3′; antisense 3′dTdT ACGUCACUACAAAGAACCU5′. siRNA was cotransfected at a concentration of 50 nmol with PEDV ORF3 expression plasmid (0.5 ng) into Vero cells in a 24-well plate. An unrelated control siRNA (si-NC) was included in the experiment as the negative control. After culture for 48 h, the effects of siRNA in suppressing PEDV ORF3 expression were determined by Western blot assay using anti-HA antibody. Vero cells used for virus infection were first transfected with siRNAs at different concentration by using Lipofectamine 2000 (Invitrogen) before being infected with the virus. After incubation for 6 h, cells were infected with PEDV at a multiplicity of infection (MOI) of 0.1. Forty eight hours after infection, cells and culture supernatants were collected for viral production measurement.

2.8. Measuring virus production

Virus production was determined using two methods. First, viral genomic RNA copies in culture supernatants were detected through real-time quantitative RT-PCR. RNA was collected using Trizol (Invitrogen). Copies of viral RNA were determined by real time PCR using the Qiagen One Step RT-PCR Kit in triplicate. The PEDV N gene was amplified using the primer pairs PEDV sense: GCAACAGCAGAAGCCTAAGCAG, antisense: CTTTGAGGTCACGTTCC-

TTCGA. Second, amounts of infectious PEDV particles were measured via $TCID_{50}$ assay.

3. Results

3.1. Structure prediction and computational modeling of PEDV OFR3 protein

To predict TMD of the ORF3, five different programs were used including DAS [20], TMHMM [21], TMpred [22], MPEx (http://blanco.biomol.uci.edu/mpex) and TopPred [23]. Based on these results, helices are assumed to be: TM1 (Gln-40 to Ser-63), TM2 (Arg-75 to Ile-97), TM3 (Tyr-116 to Tyr-139) and TM4 (Gly-150 to Ile-173) (Fig. 1A). The four helices were then assembled in a concerted fashion to form the monomer. Bundles formed by assembling in a concerted fashion from the monomers (Fig. 1B) (11). A feature all bundles shared was helix 4 facing the pore. His-152 in TMD4 was located on an interhelical face. Tyrosines and phenylalanines appeared to be randomly distributed in all models. This finding was also observed in a side view of the bundle (Fig. 1C). Notably,

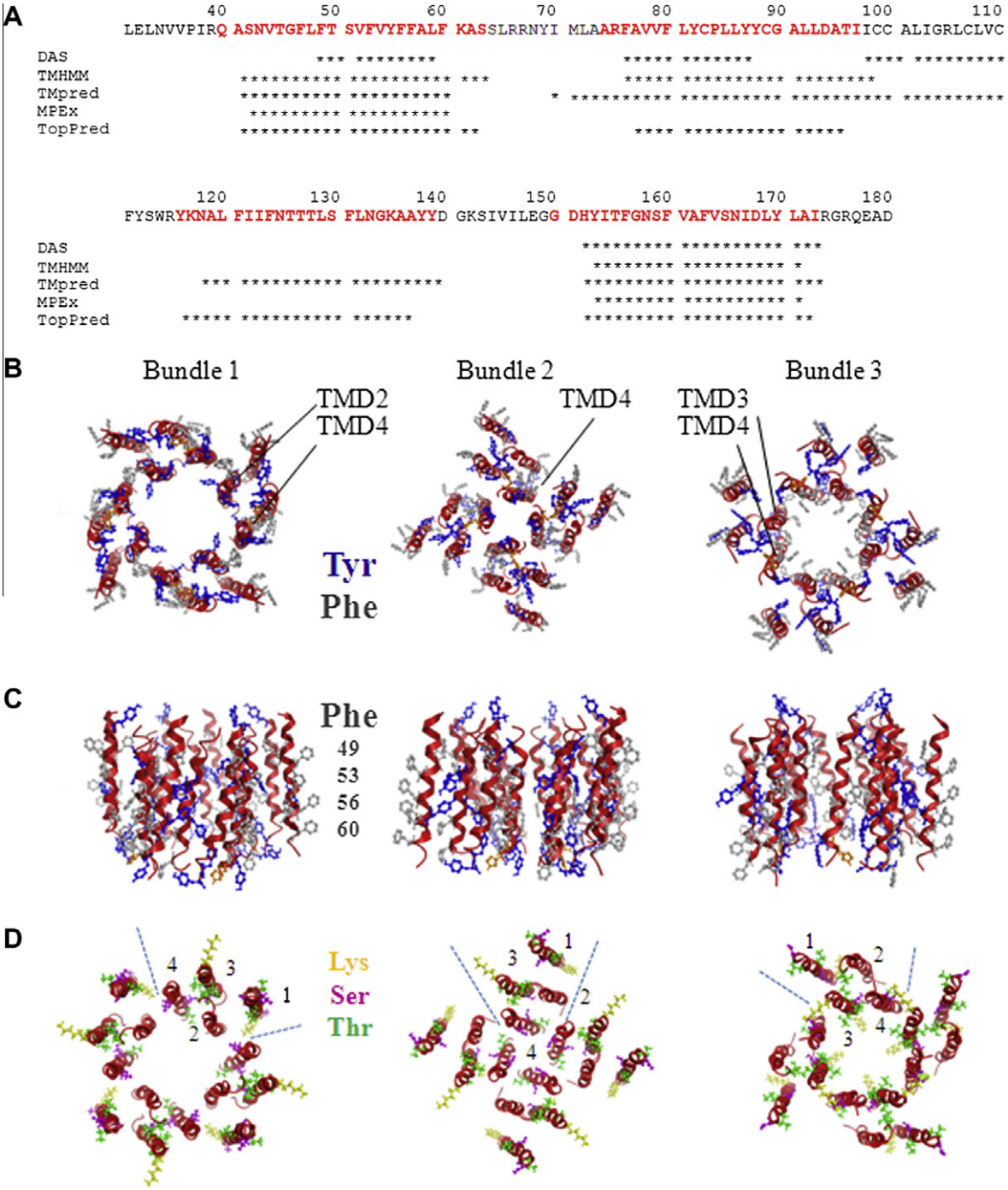

Fig. 1. Structure prediction and computational modeling of PEDV OFR3 protein. Prediction of the transmembrane (TM) parts of ORF3 protein from porcine epidemic diarrhea virus (PEDV) CV777 using different secondary structure prediction programs (A). Residues highlighted in red reflect the consensus sequence and were used for molecular dynamics (MD) simulations and assembly. Representation of three PEDV ORF3 protein assemblies with the lowest potential energy on the left (B) and second (C) and third lowest models (D). View onto the bundle with tyrosines (blue) and phenylalanines (grey) highlighted (top row). Respective side views are shown in the middle panel. Top view of the bundles with Lys-55 (yellow), serines (pink) and threonines (green) highlighted.

a line of four phenylalanines (Phe-49, -53, -56, -60) in TMD1 faced the lipid membrane (Fig. 1C). Serines and threonines (helix 4) face the pore in bundle 1, whilst in bundle 3 threonines and lysines (helix 3) point towards the center (Fig. 1D). Based on the computational design of this experiments we propose that helix 4 is the most likely helix to be involved in the formation of the pore.

3.2. PEDV ORF3 gene is functionally expressed in Xenopus oocytes and enhances membrane current

Since we predicted that ORF3 may be a transmembrane protein, we used a PEDV ORF3-specific polyclonal antibody to detect its expression in viral infected Vero cells. The PEDV CV777 strain has a 675 bp open reading frame – ORF3 between S and E gene, which encodes 224 amino acids. Western immunoblot showed that a protein of apparent molecular mass of 26 kDa is found in the PEDV CV777 infected cells, but not in the mock infected Vero cells (Fig. 2A).

We previously demonstrated that 3a protein of SARS-CoV forms an ion channel which permits potassium ions to pass through the cell membrane [10]. To investigate whether PEDV ORF3 has a similar function, PEDV ORF3 cRNAs obtained by in vitro transcription were microinjected into *X. laevis* oocytes and the trans-membrane currents measured using the two electrode voltage clamp (TEVC) technique. Both ORi and high potassium solutions were used as bath solutions. HA tagged PEDV ORF3 protein expression was revealed on oocyte cell membranes through confocal microscopy (Fig. 2B). The TEVC data showed that when oocytes express PEDV CV777 ORF3, membrane current increased obviously compared to the oocytes injected with water (Fig. 2C). Furthermore, in 100 mM potassium solution, oocytes expressing PEDV CV777 ORF3 show much larger currents than that in ORi (containing 90 mM NaCl, 2 mM KCl) solution. These data suggest that PEDV ORF3 protein may be permeable to potassium ions. When a potassium channel inhibitor, $BaCl_2$ was applied, the ORF3 mediated current was inhibited (Fig. 2D). PEDV ORF3 protein clearly has an ion channel function, with a preference for potassium ions.

To further confirm potassium ion channel activity we used yeast complementation assays to test whether the PEDV ORF3 could function as a plasma membrane K^+ channel. A potassium uptake-deficient strain of *S. cerevisiae* (W303, trk1Δ trk2Δ) can grow normally on media containing 100 mM K^+, but it cannot grow on low potassium media (7 mM K^+). However, the growth of Δtrk1trk2 knockout yeast in low-K^+ medium can be rescued by exogenous potassium channel expression. Our data shows that all yeasts grew well on a medium with a high K^+ concentration. In contrast, yeast transformed with the pYES2 vector failed to grow on a low-K^+ medium, and yeast transformed with pYES2-ORF3 did

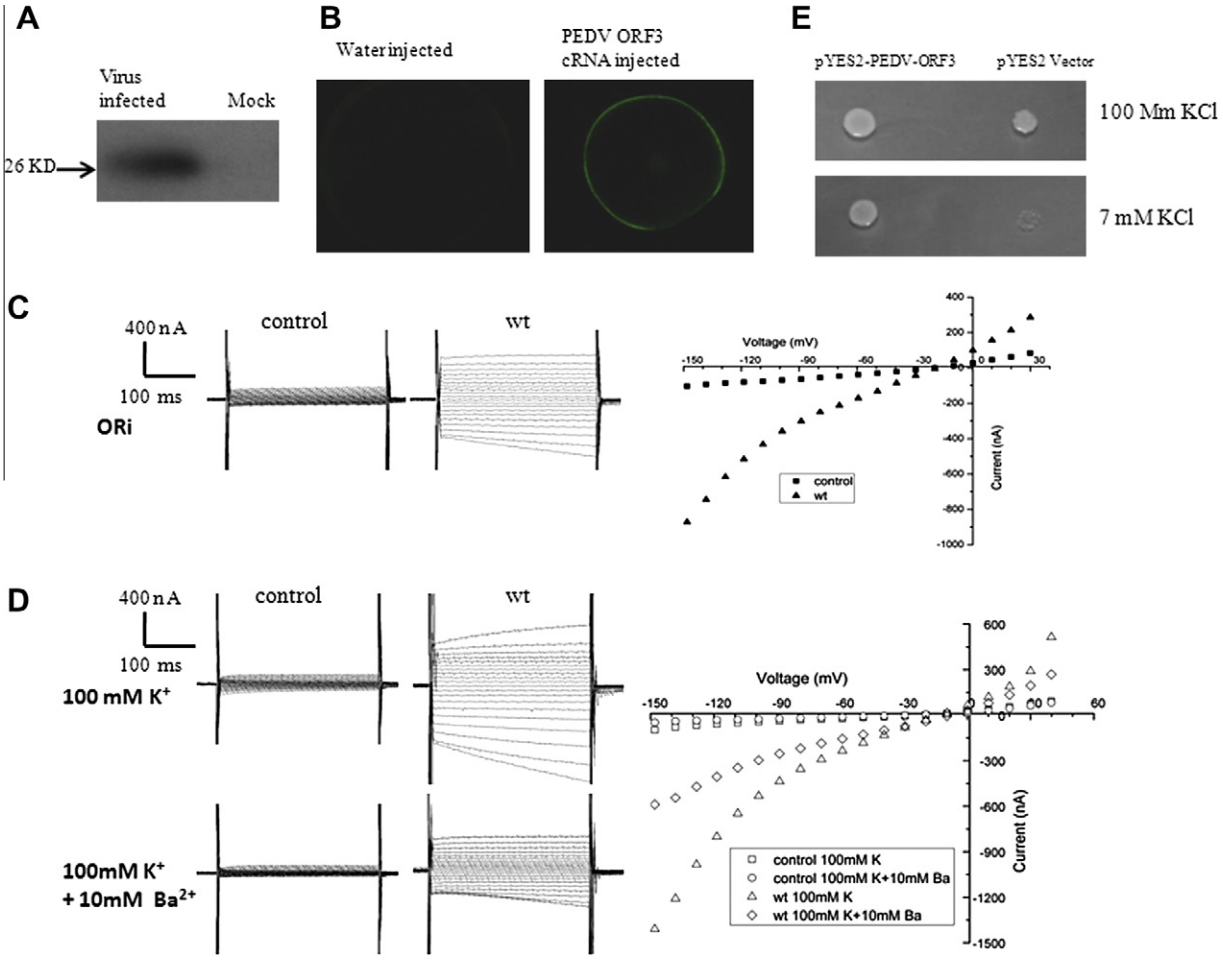

Fig. 2. The PEDV CV777 ORF3 protein forms an ion channel. (A) ORF3 protein was tested in PEDV infected cells by western blot. (B) Water-injected and PEDV ORF3-cRNA-injected oocytes are immunolabeled with anti-HA and monitored by confocal microscopy. (C) Typical current traces that can be detected by two-electrode voltage clamp (TEVC) in these PEDV CV777 ORF3 (wt) expressed oocytes, compared with water injected control oocytes. (D) PEDV CV777 ORF3 (wt) shows larger current in 100 mM K^+ bath solution than in barium ions containing standard bath solution. (E) PEDV ORF3 channel can complement K^+ channel deficient yeast. Growth phenotype of yeast Δtrk1Δtrk2 mutants transformed with PEDV CV777 ORF3 genes and pYES2 vector, respectively.

grow (Fig. 2E). These yeast K^+ uptake complementation results are consistent with the trace obtained using TEVC above. Therefore, it appears that the PEDV ORF3 coded protein forms an active plasma membrane potassium ion channel.

3.3. Deletion and mutation analysis of the ORF3

Following the output from TMpred, a series deletion across TM 1-4 was constructed. The proteins with either amino acids deleted at positions 40–63 in TM1 (40-63del), 82–98 in TM2 (82-98del), 118–136 in TM3 (118-139del) or 151–172 in TM4 (151-172del) were constructed and potassium channel activity tested in K^+ uptake deficient yeast (Fig. 3A). We found that genes with these four deletions could not rescue the growth of mutant yeast in low-K^+ medium, which imply these TM domains have an important function in potassium ion channel activity.

Consistent with the results of yeast K^+ uptake complementation experiments, the 82-98del and 151-172del protein lost ion channel activity in *X. laevis* oocytes tested under TEVC (Fig. 3B). To define which amino acid is crucial, based on the computer modeling analysis, few amino acids (His-152, Ser-159, Phe-163, Ser165, Asp-168 and Tyr-170) in TM4 are mutated to Ala. Their potassium ion channel activity was tested in both yeast and oocytes systems. We found that amino acid Y170 is very important for potassium channel activity (Fig. 3C). In conclusion, PEDV CV777 ORF3 protein plays a role in ion channel activity.

3.4. The ion channel activity is reduced in ORF3 protein of attenuated-type PEDV

It is well documented that attenuated-type PEDVs exhibit reduced pathogenicity in pigs, and a large deletion region is present in all PEDV live vaccine strains [9]. It was interesting to observe that the ORF3 gene of an attenuated-type virus has 49 nucleotide deletions, leading to a reading frame-shift and TAG terminator at 274nt. Thus, attenuated PEDV ORF3 encodes a truncated protein of 91 amino acids that lacks the TM3 (116–139aa) and TM4 (151–172aa) domains, compared to the 224 amino acids of

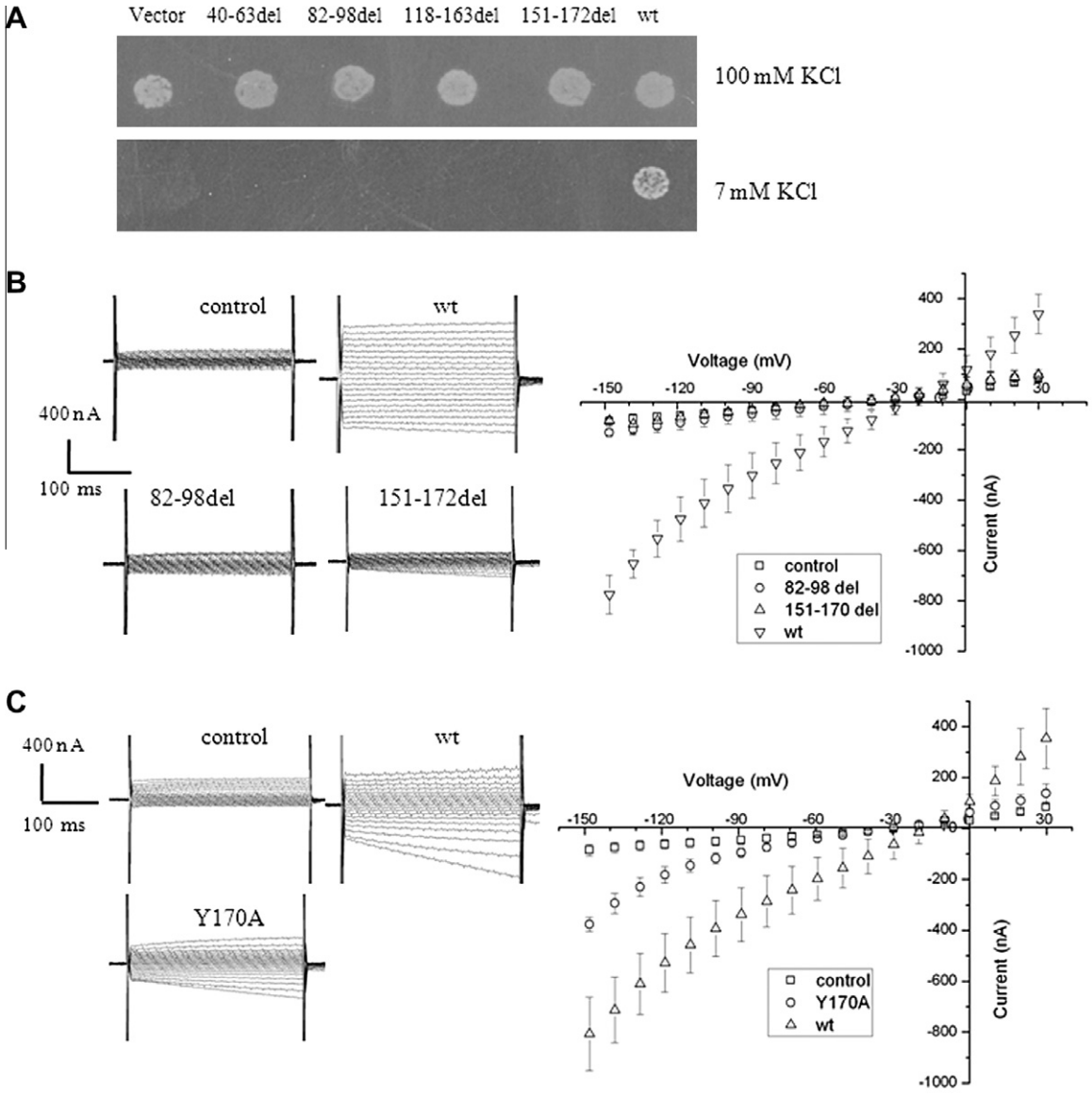

Fig. 3. Deletion and mutation analysis of PEDV ORF3 gene. (A) TM truncated ORF3 could not complement the growth phenotype of the potassium uptake-deficient yeast. (B) 82-98del and 151-172del mutant proteins lost channel activity in oocytes. (C) Tyr-170 in TM4 domain is important for potassium channel activity. Y170A (a single amino acid Tyr-170 replaced by alanine in TM4 domain) mutant shows only half the wild-type current, on average. Wt stands for wild-type PEDV ORF3.

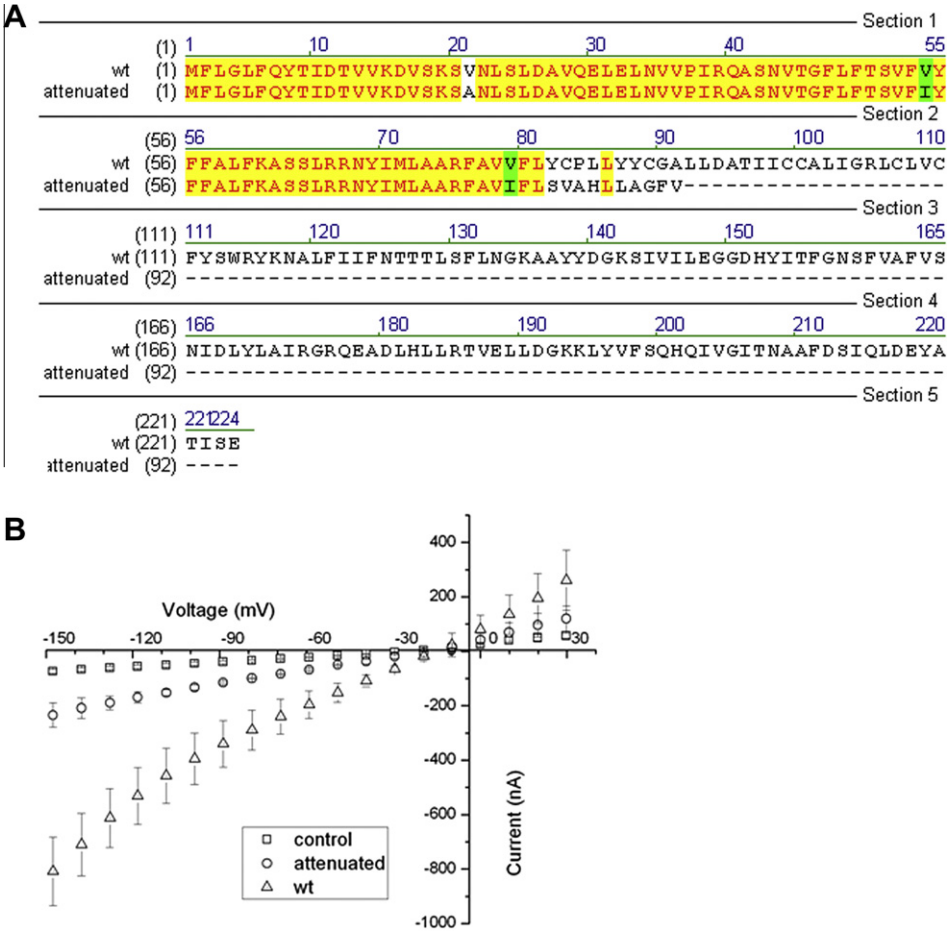

Fig. 4. The ORF3 gene of an attenuated-type PEDV encodes a truncated protein and shows less channel activity. (A) Sequence alignment of Vector NTI 9.0 with PEDV. (B) Current–voltage relationships of wild-type CV777 and attenuated-type PEDV ORF3 mediated ionic currents in oocytes by TEVC.

wild-type PEDV (Fig. 4A). In the TEVC experiments, the current activity was determined in the ORF3 genes from attenuated and wild-type PEDV. The results showed that the mean steady-state current at −150 mV was −200 nA for truncated ORF3 coded by attenuated PEDV expressed in *X. laevis* oocytes in 100 mM potassium solution, while the wild-type PDEV ORF3 had a current of −800 nA (Fig. 4B). These results suggested that wild-type ORF3 functions as an ion channel protein and may be involved in the pathogenesis of the disease infection.

3.5. The suppression of ORF3 expression in virus infected cells inhibits wild-type PEDV production

To test whether PEDV ORF3 can regulate virus production as similar as 3a protein of SARS [10], PEDV ORF3 gene was silenced in infected cells and the intracellular and extracellular viral RNA and particles were examined accordingly. A siRNA targeted the leader-mRNA junction site of the ORF3 subgenomic mRNA (sgRNA) which can specifically knockdown the ORF3 gene was designed (Fig. 5A) and its expression in the cells was checked (Fig. 5B). When ORF3 protein expression was knocked down by siRNA in the wild-type PEDV-infected Vero cells, the number of copies of viral genomic RNA in the cell culture supernatant was reduced with a dose-dependent manner (Fig. 5D). The virus genome copies were reduced 4-fold compared to the control siRNA (siNC) when the highest concentration of siRNA (50 nM) was used during PEDV infection. However, the intracellular virus RNA level had no significant change (Fig. 5C). The number of infectious PEDV particles in culture supernatants determined by $TCID_{50}$ assay, and the wild-type PEDV showed a significantly decrease in infectious viral particles (Fig. 5F). However, no obvious change has been observed in the intracellular virus RNA level (Fig. 5C) and infectious viral particles of attenuated-type PEDV (Fig. 5E and F). These results suggest that the ORF3 protein of PEDV has similar a function in controlling infectious virus production as the 3a protein of SARS-CoV.

4. Discussion

The genomes of viruses are known to code for a number of ion channels, referred to as channels [24,25] or viroporins [26,27]. In addition to pathogenesis, viroporins play a role in virus assembly and release. In the Coronaviridae, it is known that the E proteins of MHV, SARS-CoV, HCoV-229E and IBV exhibit viroporin activity [28–34]. Our group has previously found that the protein 3a of SARS-CoV could form an ion channel and modulate virus release [10] and here we show that PEDV ORF3 gene also encodes an ion channel protein and regulates virus production.

Using different structure prediction programs we predicted that the ORF3 protein of wild-type PEDV CV777 contained helical TMDs from residues 40–63 (TM1), 74–97 (TM2), 118–136 (TM3) and 151–172 (TM4). However, a 91aa protein encoded by the attenuated-type PEDV ORF3 is missing TM3 and TM4. The ORF3 bundle shows features of a pore lined by hydrophilic residues such as serines, tyrosines and lysines. In the TEVC experiments, it was demonstrated that the attenuated-type PEDV ORF3 was significantly reduced current activity as compared to the wild-type.

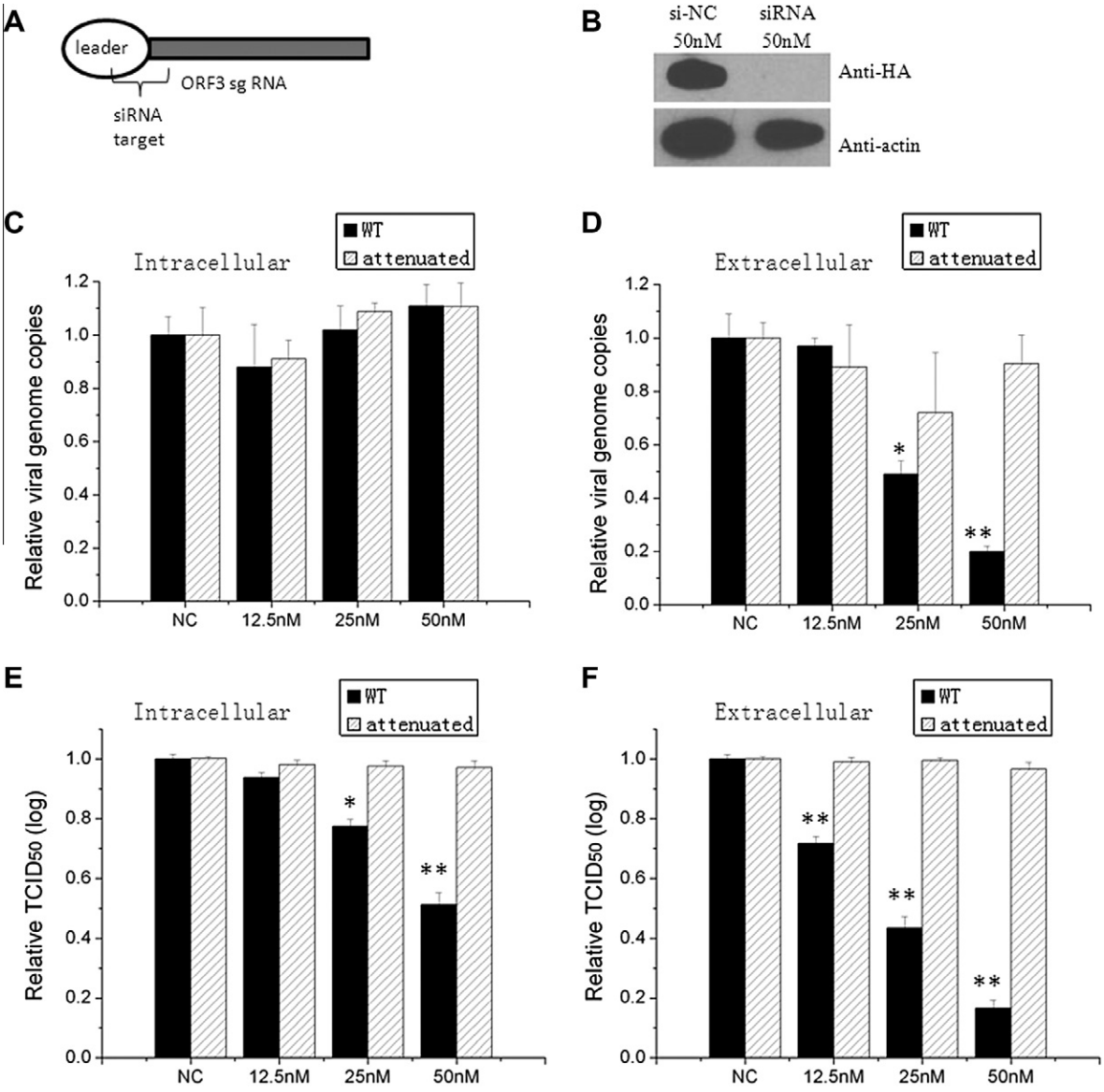

Fig. 5. The virus production is reduced on knockdown of the ORF3 gene by siRNA. (A) Schematic diagram showing the design of siRNA for knockdown of specific PEDV ORF3 subgenomic mRNA. (B) The siRNA knockdown efficiency was checked by western blotting in PEDV ORF3 expression plasmid and siRNA cotransfected cells. (C, D) The relative virus yield is quantified by real-time RT-PCR, and also titered by $TCID_{50}$ Assay (E, F). Fifty nanomolar unrelated control siRNA was used as negative control (NC), and the results from siRNA-pretreated cultures were compared with those from control transfectant (NC, defined as 100%). ($^{*}P < 0.05$, $^{**}P < 0.01$, compared with NC).

Furthermore, as the model prediction, when the residue Tyr-170 in TM4 is mutated to Ala, the potassium ion channel activity was reduced in both yeast and oocytes systems. Our proposed bundle can be used for future mutation experiments that can measure channel activity.

Seong-Jun Park et al. [9] analyzed the ORF3 gene sequence of wild-type and attenuated PEDV and found that attenuated PEDV strain DR13 has a deletion from 82 to 98aa, but this is missing from TM2 according to our prediction data. The 82-98del and truncated proteins (91aa protein encoded by the attenuated-type PEDV in our study) show less channel activity in both *X. laevis* oocytes and yeast. Only the wild-type PEDV encoding full length ORF3 protein (224aa) has high potassium channel activity. It appears that ion channel activity of the ORF3 protein is associated with the virulence of PEDV; however, the detailed mechanism of how this ion channel regulates virus production and virus pathogenesis needs further studies.

In conclusion, this study proposes a putative structural model and demonstrated the function of the PEDV ORF3 protein. It may be an appropriate drug target against coronaviruses. Further study of the PEDV ORF3 gene may also help us to understand the role it plays in PEDV infection.

Acknowledgments

We thank Deubel Vincent and Ben Bravery for reviewing the manuscript. Richard F. Gaber kindly supplied the K^+ uptake-deficient yeast strain. This work was supported by grants from CAS (KSCX2-YW-R-161, KSCX2-YW-R-169, KSCX2-EW-J-14), National Ministry of Science and Technology (2007DFC31700), National Natural Science Foundation of China(30950002, 30623003, 30721065, 30801011, 30870126, 90713044), National Science and Technology Major Project (2009ZX10004-016, 2008ZX10004-002, 2009ZX10004-105), National 973 key project (2007CB512404), grants from SPHRF

(SPHRF2008001, SPHRF2009001), National 863 project (2006AA 02A247), and Li Kha Shing Foundation.

References

[1] Kocherhans, R., Bridgen, A., Ackermann, M. and Tobler, K. (2001) Completion of the porcine epidemic diarrhoea coronavirus (PEDV) genome sequence. Virus Genes 23, 137–144.
[2] Debouck, P., Pensaert, M. and Coussement, W. (1981) The pathogenesis of an enteric infection in pigs, experimentally induced by the coronavirus-like agent, CV777. Vet. Microbiol. 6, 157–165.
[3] Zeng, R. et al. (2004) Characterization of the 3a protein of SARS-associated coronavirus in infected Vero E6 cells and SARS patients. J. Mol. Biol. 341, 271–279.
[4] Song, D.S., Yang, J.S., Oh, J.S., Han, J.H. and Park, B.K. (2003) Differentiation of a Vero cell adapted porcine epidemic diarrhea virus from Korean field strains by restriction fragment length polymorphism analysis of ORF 3. Vaccine 21, 1833–1842.
[5] Duarte, M., Tobler, K., Bridgen, A., Rasschaert, D., Ackermann, M. and Laude, H. (1994) Sequence analysis of the porcine epidemic diarrhea virus genome between the nucleocapsid and spike protein genes reveals a polymorphic ORF. Virology 198, 466–476.
[6] Bridgen, A., Kocherhans, R., Tobler, K., Carvajal, A. and Ackermann, M. (1998) Further analysis of the genome of porcine epidemic diarrhoea virus. Adv. Exp. Med. Biol. 440, 781–786.
[7] Schmitz, A., Tobler, K., Suter, M. and Ackermann, M. (1998) Prokaryotic expression of porcine epidemic diarrhoea virus ORF3. Adv. Exp. Med. Biol. 440, 775–780.
[8] Utiger, A., Tobler, K., Bridgen, A., Suter, M., Singh, M. and Ackermann, M. (1995) Identification of proteins specified by porcine epidemic diarrhoea virus. Adv. Exp. Med. Biol. 380, 287–290.
[9] Park, S.J., Moon, H.J., Luo, Y., Kim, H.K., Kim, E.M., Yang, J.S., Song, D.S., Kang, B.K., Lee, C.S. and Park, B.K. (2008) Cloning and further sequence analysis of the ORF3 gene of wild- and attenuated-type porcine epidemic diarrhea viruses. Virus Genes 36, 95–104.
[10] Lu, W. et al. (2006) Severe acute respiratory syndrome-associated coronavirus 3a protein forms an ion channel and modulates virus release. Proc. Natl. Acad. Sci. USA 103, 12540–12545.
[11] Siqi, M., Ming, W., Jinfa, Z. and Li, F. (1994) Adaption of porcine epidemic diarrhea virus to growth in cell cultures and efficacy of the killed virus vaccine. Chin. J. Prev. Vet. Med. 75, 15–19.
[12] Hofmann, M. and Wyler, R. (1988) Propagation of the virus of porcine epidemic diarrhea in cell culture. J. Clin. Microbiol. 26, 2235–2239.
[13] Tong, Y.E., Feng, Li, Li, W.J., Wang, M. and Ma, S.Q. (1998) Development of porcine epidemic diarrhea attenuated virus. Chin. J. Anim. Poult. Infect. Dis. 20, 329–332.
[14] Kruger, J. and Fischer, W.B. (2009) Assembly of viral membrane proteins. J. Chem. Theory Comput. 5, 2503–2513.
[15] Plugge, B. et al. (2000) A potassium channel protein encoded by chlorella virus PBCV-1. Science 287, 1641–1644.
[16] Nakamura, R.L., Anderson, J.A. and Gaber, R.F. (1997) Determination of key structural requirements of a K+ channel pore. J. Biol. Chem. 272, 1011–1018.
[17] Akerstrom, S., Mirazimi, A. and Tan, Y.J. (2007) Inhibition of SARS-CoV replication cycle by small interference RNAs silencing specific SARS proteins, 7a/7b, 3a/3b and S. Antiviral Res. 73, 219–227.
[18] Tobler, K. and Ackermann, M. (1995) PEDV leader sequence and junction sites. Adv. Exp. Med. Biol. 380, 541–542.
[19] Reynolds, A., Leake, D., Boese, Q., Scaringe, S., Marshall, W.S. and Khvorova, A. (2004) Rational siRNA design for RNA interference. Nat. Biotechnol. 22, 326–330.
[20] Cserzo, M., Wallin, E., Simon, I., von Heijne, G. and Elofsson, A. (1997) Prediction of transmembrane alpha-helices in prokaryotic membrane proteins: the dense alignment surface method. Protein Eng. 10, 673–676.
[21] Sonnhammer, E.L., von Heijne, G. and Krogh, A. (1998) A hidden Markov model for predicting transmembrane helices in protein sequences. Proc. Int. Conf. Intell. Syst. Mol. Biol. 6, 175–182.
[22] Hofmann, K. and Stoffel, W. (1993) TMbase – a database of membrane spanning proteins segments. Biol. Chem. Hoppe-Seyler 347, 166.
[23] von Heijne, G. (1992) Membrane protein structure prediction. hydrophobicity analysis and the positive-inside rule. J. Mol. Biol. 225, 487–494.
[24] Fischer, W.B. and Hsu, H.J. (2011) Viral channel forming proteins – modeling the target. Biochim. Biophys. Acta. 1808, 561–571.
[25] Wang, K., Xie, S. and Sun, B. (2011) Viral proteins function as ion channels. Biochim. Biophys. Acta. 1808, 510–515.
[26] Gonzalez, M.E. and Carrasco, L. (2003) Viroporins. FEBS Lett. 552, 28–34.
[27] Madan, V., Castello, A. and Carrasco, L. (2008) Viroporins from RNA viruses induce caspase-dependent apoptosis. Cell Microbiol. 10, 437–451.
[28] Madan, V., Garcia Mde, J., Sanz, M.A. and Carrasco, L. (2005) Viroporin activity of murine hepatitis virus E protein. FEBS Lett. 579, 3607–3612.
[29] Liao, Y., Yuan, Q., Torres, J., Tam, J.P. and Liu, D.X. (2006) Biochemical and functional characterization of the membrane association and membrane permeabilizing activity of the severe acute respiratory syndrome coronavirus envelope protein. Virology 349, 264–275.
[30] Liao, Y., Lescar, J., Tam, J.P. and Liu, D.X. (2004) Expression of SARS-coronavirus envelope protein in *Escherichia coli* cells alters membrane permeability. Biochem. Biophys. Res. Commun. 325, 374–380.
[31] Wilson, L., McKinlay, C., Gage, P. and Ewart, G. (2004) SARS coronavirus E protein forms cation-selective ion channels. Virology 330, 322–331.
[32] Wilson, L., Gage, P. and Ewart, G. (2006) Hexamethylene amiloride blocks E protein ion channels and inhibits coronavirus replication. Virology 353, 294–306.
[33] Ye, Y. and Hogue, B.G. (2007) Role of the coronavirus E viroporin protein transmembrane domain in virus assembly. J. Virol. 81, 3597–3607.
[34] Pervushin, K. et al. (2009) Structure and inhibition of the SARS coronavirus envelope protein ion channel. PLoS Pathog. 5, e1000511.